

Identification mechanism of BACE1 on inhibitors probed by using multiple separate molecular dynamics simulations and comparative calculations of binding free energies

Yi Wen Wang^{1,2}, Fen Yang¹, Dongliang Yan^{1,3}, Yalin Zeng¹, Benzheng Wei⁴, Jianzhong Chen^{1,3*} and Weikai He^{1,2*}

¹ School of Information Science and Electrical Engineering, Shandong Jiaotong University, Jinan, 250357, China

² School of Aeronautics, Shandong Jiaotong University, Jinan, Shandong, China, 250357, China

³ School of Science, Shandong Jiaotong University, Jinan, 250357, China

⁴ Center for Medical Artificial Intelligence, Shandong University of Traditional Chinese Medicine, Qingdao, 266112, China

*Correspondence: 214035@sdjtu.edu.cn(W.H.), chenjianzhong1970@163.com (J.C.); jzchen@sdjtu.edu.cn (J.C.)

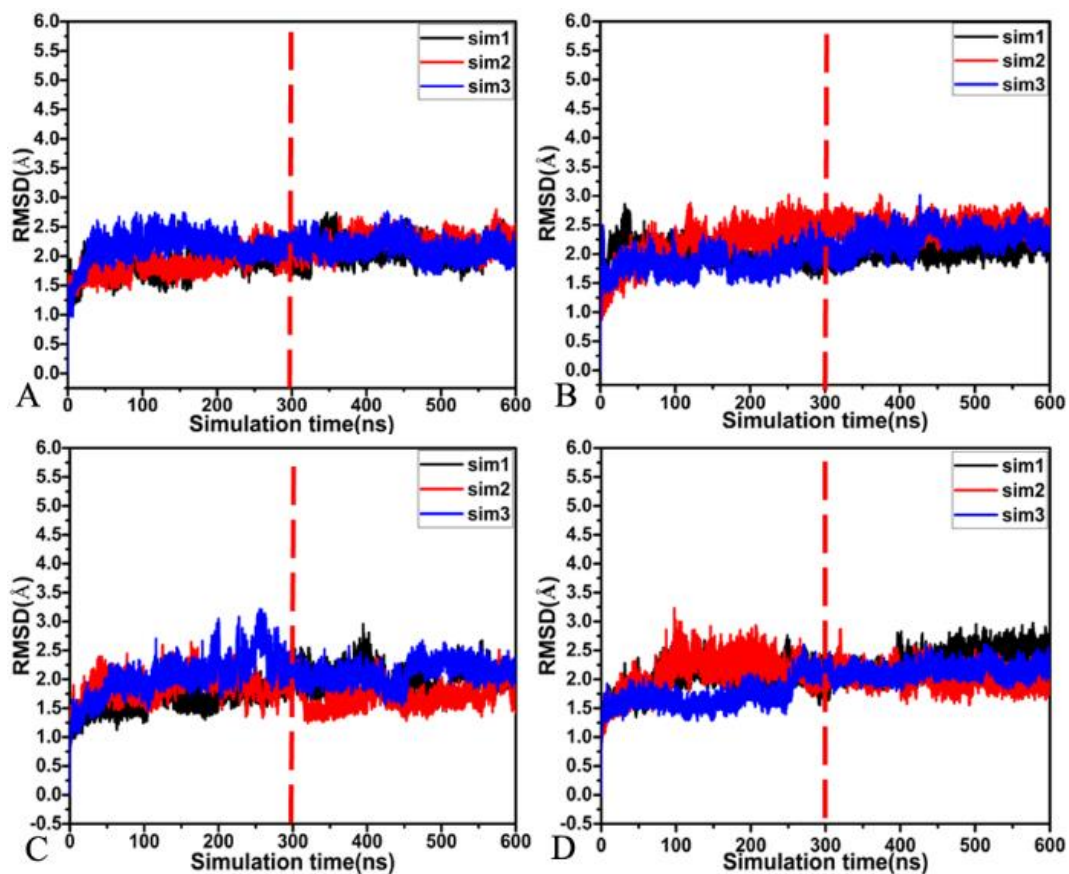


Figure S1. RMSDs of backbone atoms in BACE1 calculated by using three separate MD trajectories: (A) the *apo* BACE1, (B) the 60W-BACE1 complex, (C) the 954-BACE1 complex and (D) the 60X-BACE1 complex.

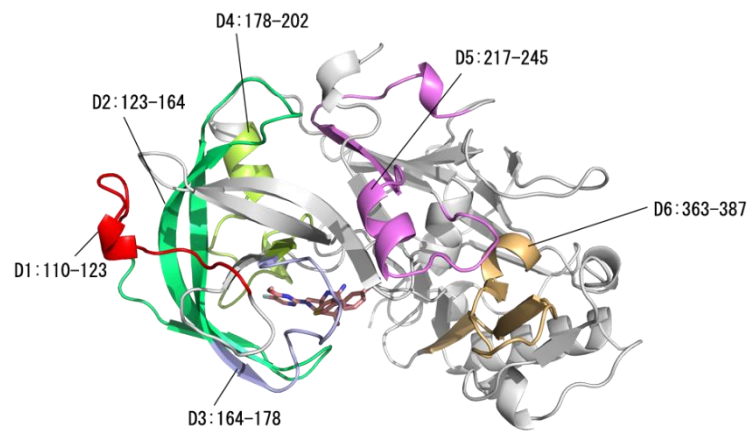


Figure S2. Structural domains corresponding to the obvious changes in RMSFs due to inhibitor binding.

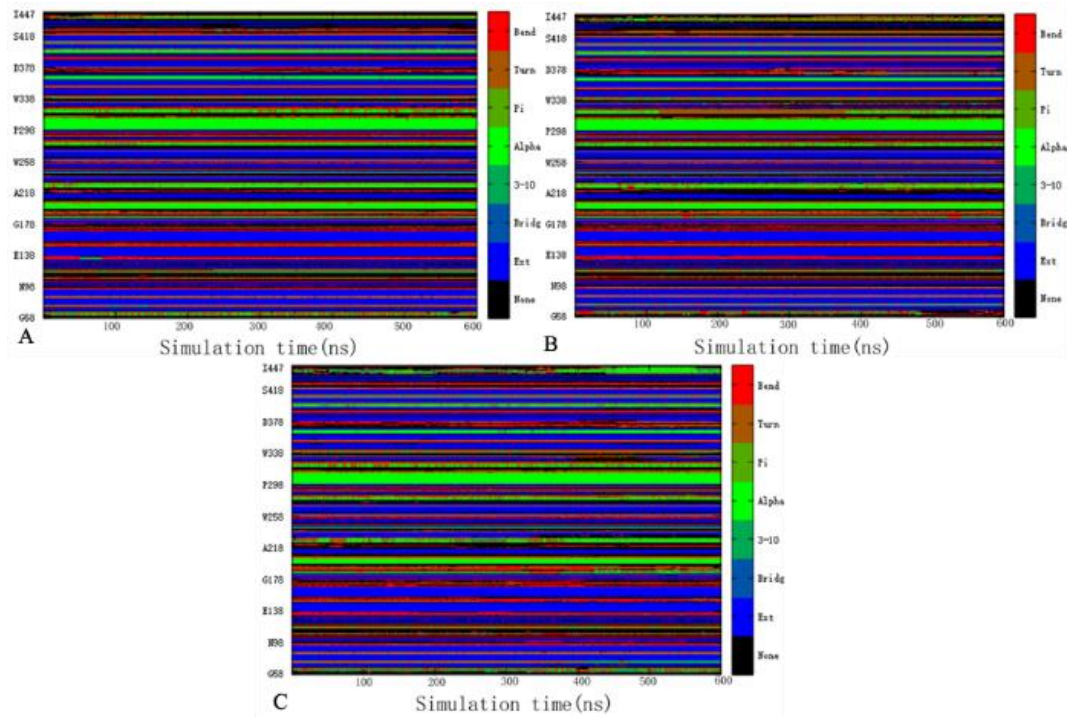


Figure S3. Stability of secondary structures for the 60W-bound BACE1 in three separate MD simulations: (A) the simulation 1, (B) the simulation 2 and (C) the simulation 3.

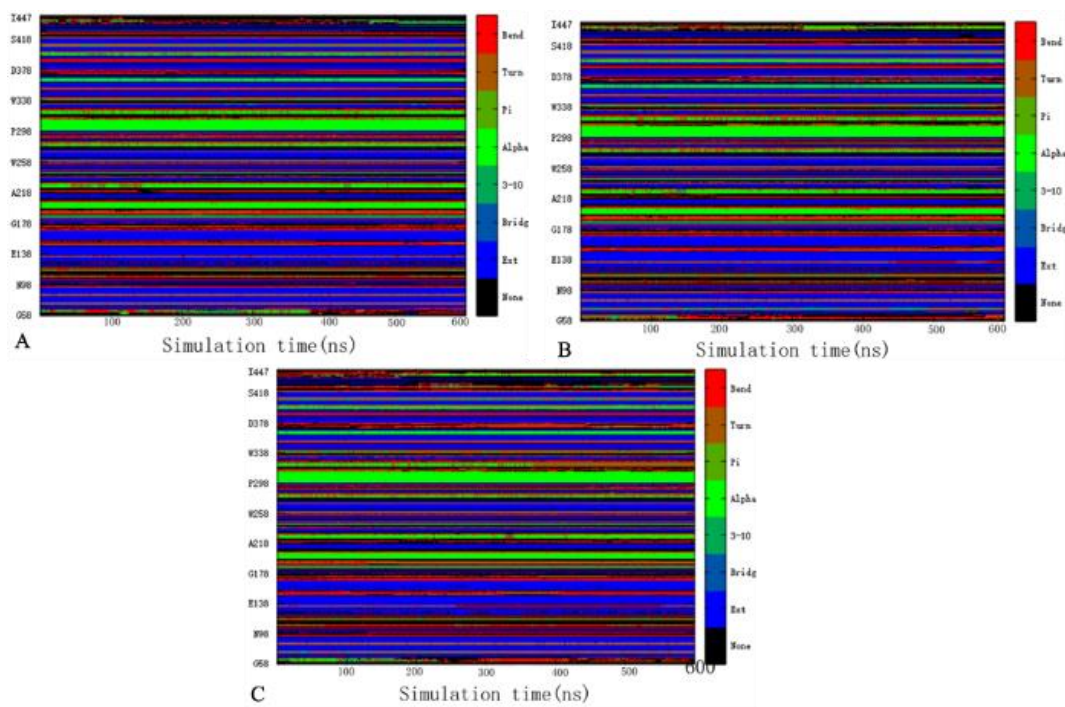


Figure S4. Stability of secondary structures for the 954-bound BACE1 in three separate MD simulations: (A) the simulation 1, (B) the simulation 2 and (C) the simulation 3.

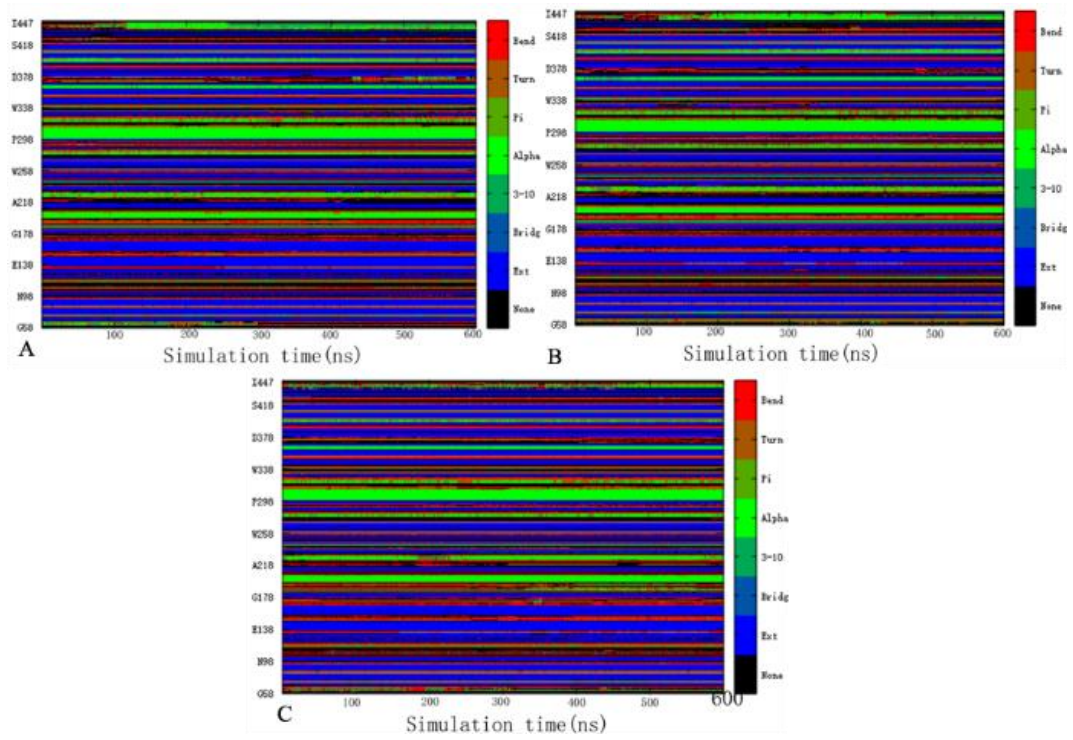


Figure S5. Stability of secondary structures for the 60X-bound BACE1 in three separate MD simulations: (A) the simulation 1, (B) the simulation 2 and (C) the simulation 3.

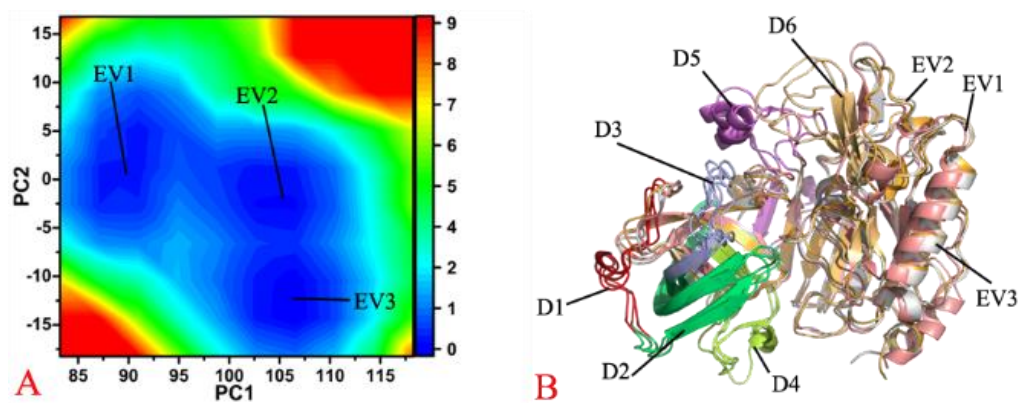


Figure S6. (A) Free energy landscapes of the *apo* BACE1 constructed by using the PC1 and PC2 as reaction coordinates and (B) structural superimposition of the *apo* BACE1 situated at the energy valleys EV1-EV3.